Molecular Biology of the Cell
Vol. 16, 2544–2553, May 2005

Atg17 Functions in Cooperation with Atg1 and Atg13 in Yeast Autophagy

Yukiko Kabeya,* Yoshiaki Kamada,*†‡ Misuzu Baba,* Hirosato Takikawa,§ Mitsuru Sasaki,§ and Yoshinori Ohsumi*†

*Division of Molecular Cell Biology, National Institute for Basic Biology, Okazaki 444-8585, Japan; †School of Life Science, The Graduate University for Advance Studies, Okazaki 444-8585, Japan; ‡CREST, Japan Science and Technology Agency, Kawaguchi 332-0012, Japan; and §Department of Biosystems Science, Graduate School of Science and Technology, Kobe University, Kobe 657-8501, Japan

Submitted August 6, 2004; Accepted February 18, 2005
Monitoring Editor: Suresh Subramani

In eukaryotic cells, nutrient starvation induces the bulk degradation of cellular materials; this process is called autophagy. In the yeast *Saccharomyces cerevisiae*, most of the *ATG* (*aut*ophagy) genes are involved in not only the process of degradative autophagy, but also a biosynthetic process, the cytoplasm to vacuole (Cvt) pathway. In contrast, the *ATG17* gene is required specifically in autophagy. To better understand the function of Atg17, we have performed a biochemical characterization of the Atg17 protein. We found that the *atg17*Δ mutant under starvation condition was largely impaired in autophagosome formation and only rarely contained small autophagosomes, whose size was less than one-half of normal autophagosomes in diameter. Two-hybrid analyses and coimmunoprecipitation experiments demonstrated that Atg17 physically associates with Atg1-Atg13 complex, and this binding was enhanced under starvation conditions. Atg17-Atg1 binding was not detected in *atg13*Δ mutant cells, suggesting that Atg17 interacts with Atg1 through Atg13. A point mutant of Atg17, Atg17^{C24R}, showed reduced affinity for Atg13, resulting in impaired Atg1 kinase activity and significant defects in autophagy. Taken together, these results indicate that Atg17-Atg13 complex formation plays an important role in normal autophagosome formation via binding to and activating the Atg1 kinase.

INTRODUCTION

Autophagy is a membrane-trafficking process that transports bulk intracellular materials to the vacuole for degradation in response to nutrient starvation (Takeshige *et al.*, 1992; Baba *et al.*, 1997; Hutchins *et al.*, 1999). During autophagy, cytoplasmic materials are sequestered in double-membrane structures called autophagosomes, which fuse with the vacuole (Baba *et al.*, 1994). The inner membrane structures of autophagosomes are delivered to the vacuole as autophagic bodies (Baba *et al.*, 1994). The autophagic bodies are then disrupted by hydrolases in the vacuole (Takeshige *et al.*, 1992). In yeast, autophagy is essential for survival during nitrogen starvation and for sporulation (Tsukada and Ohsumi, 1993).

Genetic analysis of autophagy mutants in *Saccharomyces cerevisiae* revealed an overlap with genes involved in the cytoplasm to vacuole targeting (Cvt) pathway that delivers the vacuolar resident hydrolases, aminopeptidase I (Ape1) and α-mannosidase (Ams1; Tsukada and Ohsumi, 1993; Thumm *et al.*, 1994; Scott *et al.*, 1996). Consistent with the significant overlap in transport machinery between the two pathways, the Cvt pathway shares common mechanistic features with autophagy, including the formation of double-membrane vesicles, called Cvt vesicles, and breakdown of single-membrane vesicles (Cvt bodies) in the vacuolar lumen (Klionsky and Ohsumi, 1999). Therefore, proApe1 (prApe1) is delivered by the Cvt pathway under nutrient-rich conditions and transported by autophagy under starvation conditions, allowing the maturation of prApe1 to the mature form.

Autophagosomes (300–900 nm in diameter) are substantially larger than Cvt vesicles (140–160 nm; Baba *et al.*, 1997). For autophagosome formation, a corresponding increase in membrane materials is likely to be required. The characterization of additional factors, such as autophagy-specific proteins that mediate the process of membrane sequestration, is still lacking.

An important role in switching from the Cvt pathway to autophagy in response to nutrient conditions seems to be mediated by the Atg1-Atg13 complex. Atg1 is a protein kinase and is required for both autophagy and the Cvt pathway (Scott *et al.*, 1996; Matsuura *et al.*, 1997; Straub *et al.*, 1997). During growth conditions, Atg13 is hyperphosphorylated in a Tor-dependent manner and has reduced affinity for Atg1 (Kamada *et al.*, 2000). On a shift to starvation conditions or with rapamycin treatment (specific inhibitor of Tor), Atg13 is rapidly dephosphorylated, which increases the affinity of Atg13 for Atg1, and leads to induction of autophagy (Funakoshi *et al.*, 1997; Matsuura *et al.*, 1997; Kamada *et al.*, 2000). Based on our previous results, binding of dephosphorylated Atg13 to Atg1 enhances the kinase activity of Atg1, which was proposed to switch the vesicle formation machinery from the Cvt pathway to autophagy (Kamada *et al.*, 2000). However, recent studies using chem-

This article was published online ahead of print in *MBC in Press* (http://www.molbiolcell.org/cgi/doi/10.1091/mbc.E04–08–0669) on March 2, 2005.

Address correspondence to: Yoshinori Ohsumi (yohsumi@nibb.ac.jp).

Abbreviations used: ALP, alkaline phosphatase (Pho8); ATG genes, autophagy-related genes; Cvt, cytoplasm to vacuole targeting; HA, hemagglutinin.

Table 1. Yeast strains used in this study

Strain	Genotype	Source
BJ2168	*MAT***a** *leu2 trp1 ura3 pep4-3 prb1-1122 prc1-407*	Yeast Genetic Stock Center
YYK200	BJ2168 *atg17*Δ*::kanMX*	This study
YYK416	BJ2168 *ATG1::HA-ATG1 atg17*Δ*::kanMX*	This study
YYK422	BJ2168 *ATG1::HA-ATG1 ATG17::FLAG-ATG17*	This study
YYK426	BJ2168 *ATG1::HA-ATG1 ATG17::FLAG-ATG17 atg13*Δ*::kanMX*	This study
YYK424	BJ2168 *atg1*Δ*::LEU2 ATG17::FLAG-ATG17*	This study
YYK467	BJ2168 *ATG1::HA-ATG1 ATG17::FLAG-atg17*^{C24R}	This study
SEY6210	*MAT*α *his3 leu2 lys2 trp1 ura3 suc2*	Robinson *et al.* (1988)
KVY55	SEY6210 *pho8::pho8*Δ*60*	Kirisako *et al.* (1999)
YTS007	KVY55 *atg9*Δ*::kanMX*	This study
YYK382	KVY55 *atg17*Δ*::kanMX*	This study
YYK475	KVY55 *atg11*Δ*::URA3*	This study
YYK381	SEY6210 *pep4*Δ*::LEU2 atg17*Δ*::kanMX*	This study
KA311A	*MAT***a** *his3 leu2 trp1 ura3*	Irie *et al.*, (1993)
YYK36	KA311A *atg1*Δ*::LEU2*	Kamada *et al.* (2000)
YYK111	KA311A *atg17*Δ*::HIS3*	Kamada *et al.* (2000)
PJ69–4A	*MAT***a** *his3-200 leu2-3, 112 trp1-901 ura3-52 gal4*Δ *gal80*Δ *GAL2-ADE2 LYS2::GAL1-HIS3 met2::GAL7-lacZ*	James *et al.* (1996)
TN124	*MAT***a** *ura3 trp1 pho8::pho8*Δ*60 pho13::LEU2*	Noda *et al.* (1995)
TN124–1C	TN124 *atg1-1*	This study
TN125	*MAT***a** *ade2 his3 leu2 lys2 trp1 ura3 pho8::pho8*Δ*60*	Noda *et al.* (1995)
TN126	TN125 *atg1*Δ*::LEU2*	Kamada *et al.* (2000)

ical genetics to allow in vivo assessment of the role of Atg1 kinase activity have suggested that kinase activity is required for the Cvt pathway but not for autophagy (Abeliovich *et al.*, 2003). To clarify this discrepancy, we have reinvestigated the requirement of Atg1 kinase activity for autophagy through the characterization of Atg17, which is a specific component of the autophagic pathway.

ATG17 was first identified by a two-hybrid screen using *ATG1* as bait (Kamada *et al.*, 2000). *ATG17* is required specifically for autophagy, but its precise role remains to be determined. The fact that overexpression of Atg1 rescues the autophagic defect in *atg17*Δ cells suggests that Atg17 acts upstream of Atg1. Furthermore, the null mutation of *ATG17* largely impaired Atg1 kinase activity, implying that Atg17 is also involved in Atg1 kinase activation (Kamada *et al.*, 2000).

Here, we demonstrate that Atg17 forms complex with Atg1-Atg13 under control of Tor. This complex is required for proper autophagosome formation directed by Atg1 kinase activity.

MATERIALS AND METHODS

Yeast Strains and Media

Media for growth of yeast cells, starvation, and induction of autophagy have been described previously (Kaiser *et al.*, 1994; Kamada *et al.*, 2000). We used standard methods and media for yeast manipulation (Kaiser *et al.*, 1994). *S. cerevisiae* strains used in this study are listed in Table 1. The *atg13*Δ*::KanMX* and *atg17*Δ*::KanMX* mutants were constructed as follows. Regions containing the disruption marker and the flanking sequences were PCR amplified using genomic DNA prepared from BY4741 *atg13*Δ*::KanMX* or *atg17*Δ*::KanMX* strains (Giaever *et al.*, 2002). The *atg1*Δ strain was constructed according to the previously described method (Matsuura *et al.*, 1997). All primer sequences will be made available upon request. Vacuolar morphology and autophagic body accumulation were microscopically observed to confirm normal function of both integrated HA-tagged *ATG1* and FLAG-tagged wild-type *ATG17*.

Plasmid Construction

The *ATG17* gene was cloned into the *Spe*I and *Sph*I sites of pRS306 by amplifying the open reading frame plus 400 bases upstream of the initiation codon and 600 bases downstream of the termination codon using primers containing *Spe*I and *Sph*I sites. The FLAG-tagged *ATG17* construct was engineered by first creating a *Not*I site by insertion of the tag immediately after the first methionine codon by QuikChange (Stratagene, La Jolla, CA). Then the 3× FLAG *Not*I cassette was inserted into the newly created *Not*I site.

For a two-hybrid assay, the entire *ATG17* ORF was amplified by PCR and inserted into the *Eco*RI site of pGAD-C1 (James *et al.*, 1996) to generate pGAD[*ATG17*], which expresses Atg17 fused to the Gal4 activation domain. pGBD[*ATG13*] was created by subcloning the entire *ATG13* coding sequence into the *Bgl*II and *Xba*I sites of pGBD-C_1; the resulting plasmid expressing the DNA-binding domain of Gal4 fused to Atg13. pGBD[*ATG1*^{K54R}] used to identify originally *ATG17* from a two-hybrid screen was described previously (Kamada *et al.*, 2000).

The plasmid for expression of FLAG-tagged Atg17 with a point mutation changing the Cys at position 24 to Arg (Atg17^{C24R}) was generated by PCR-based site-directed mutagenesis.

Electron Microscopy

Cells were subjected to rapid freezing and freeze-substitution fixation, and observed as previously reported (Baba *et al.*, 1997).

Immunoprecipitation and Protein Kinase Assays

Yeast cells were grown exponentially in YEPD to OD_{600} = 2–4, and 100 OD_{600} units of cells were treated with zymolyase 100T (10 U/OD_{600} cell; Seikagaku Kogyo, Tokyo, Japan) in Z buffer (50 mM Tris-HCl [pH 7.5], 1 M sorbitol, 1% yeast extract, 2% polypepton, and 1% glucose) to generate spheroplasts. The resulting spheroplasts were divided into two aliquots, treated with or without 0.2 μg/ml rapamycin (Sigma, St. Louis, MO), and lysed with 0.5% Tween-20 in phosphate-buffered saline on ice as previously described (Kamada *et al.*, 2000). The cell lysates were incubated with anti-HA (16B12, BAbCo, Richmond, CA) or anti-Atg13 antibody and protein G-Sepharose at 4°C for 2 h. The immunoprecipitated proteins were separated by SDS-PAGE and analyzed by immunoblotting with mouse monoclonal antibodies against HA and FLAG (M2, Sigma) or rabbit polyclonal antibodies against Atg13 and Atg17. For each experiment, 0.5% of total cell lysate was also loaded to monitor amount of Atg proteins. Immunodetection was carried out with the ECL system (Amersham Biosciences, Piscataway, NJ) using a bioimage analyzer (LAS1000, Fujifilm, Tokyo, Japan). Anti-Atg17 antibody was obtained by immunizing a rabbit with a recombinant His_6-tagged Atg17 by Shibayagi (Gunma, Japan).

An in vitro Atg1 kinase assay was performed with myelin basic protein or recombinant Atg1 protein (donated by Dr. F. Inagaki, Hokkaido University) as a substrate as described previously (Kamada *et al.*, 2000). An autophosphorylation Atg1 assay was also underwent according to the method previously described (Matsuura *et al.*, 1997).

Screening of atg17 Mutants by Two-hybrid Analysis

The two-hybrid screening was performed using the system described previously (James *et al.*, 1996). Mutagenic PCR was conducted using pGAD-C_1[*ATG17*$^{wild\text{-}type}$] as a template to amplify mutagenized *ATG17* with the

flanking region (Dieffenbach and Dveksler, 1995). The PCR product was cotransformed with pGAD-C_1 (linearized by treatment with *Bam*HI and *Pst*I) into the strain PJ69–4A, which was transformed with either pGBD[*ATG1*^{K54R}] or pGBD[*ATG13*]. Transformants were selected for growth on SC-Leu-Trp plates and then tested for defective growth on SC-Ade-Leu-Trp plates. Ade$^-$ colonies were tested for defective growth on SC-His-Leu-Trp plates containing 5 mM 3-AT. About 100 Ade$^-$ and His$^-$ transformants were obtained as candidates from the 200 total transformants. We randomly chose several transformants, and the plasmids were rescued from 9 (*ATG1*-bait cell) and 25 (*ATG13*-bait cell) colonies. After sequencing the plasmid, we obtained 6 (*ATG1*-bait cell) and 12 (*ATG13*-bait cell) *atg17* mutant genes having several point mutations. The rest had nonsense mutation in the *ATG17* gene. The full-length Atg17 of 1 (*ATG1*-bait cell) and 4 (*ATG13*-bait cell) *atg17* mutants was detected by immunoblotting using anti-Atg17 antibody. Subsequent two-hybrid analyses were carried out by cotransformation of pGBD[*ATG1*^{K54R}] and 4 (*ATG13*-bait cell) *atg17* mutants in the pGAD vector, or pGBD[*ATG13*] and 1 (*ATG1*-bait cell) *atg17* mutant in the pGAD vector into the PJ69–4A strain. Transformants were selected on SC-Leu-Trp plates and then tested for growth on SC-Ade-Leu-Trp plates.

Synthesis of 4-Amino-1-tert-butyl-3-(1′-naphthyl)pyrazolo [3,4-d]pyrimidine (1-NA-PP1)

According to the reported procedure (Hanafeld *et al.*, 1996; Bishop *et al.*, 1999), the compound was prepared as follows. 1-naphthoyl chloride (3.8 ml, 25 mmol) and malononitrile (1.65 g, 25 mmol) were converted into (methoxy-1-naphtylmethylene)malononitrile (5.01 g, 85% yield in 2 steps). ^{1}H-NMR (300 MHz, $CDCl_3$): 3.71 (3H, s), 7.51–7.73 (5H, m), 7.97 (1H, br dd, J = 7.2, 2.1 Hz), 8.09 (^{1}H, dd, J = 7.5, 2.1 Hz); ^{13}C-NMR (75 MHz, $CDCl_3$): 60.05, 69.32, 111.29, 112.54, 123.25, 125.20, 125.31, 127.52, 128.31, 128.82, 129.19, 129.25, 133.09, 133.38, 185.30. The resulting malononitrile (2.00 g, 8.54 mmol) was then converted into 1-NA-PP1 (132 mg, 4.9% yield in 2 steps). Although the isolation yield was rather low, the obtained 1-NA-PP1 was carefully purified and was demonstrated to be pure, based on NMR analyses. ^{1}H-NMR (300 MHz, $CDCl_3$): 1.89 (9H, s), 4.92 (2H, br), 7.46–7.70 (4H, m), 7.90–8.00 (3H, m), 8.40 (1H, s); ^{13}C-NMR (75 MHz, $CDCl_3$): 29.25, 60.48, 101.44, 125.43, 125.58, 126.44, 127.03, 128.35, 128.38, 129.50, 130.54, 131.77, 133.97, 140.39, 153.80, 154.48, 157.86.

Other Methods

For measurement of autophagic activity, the alkaline phosphatase (ALP) assay was performed as described previously (Noda and Ohsumi, 1998). Cell viability was determined as described previously (Matsuura *et al.*, 1997).

RESULTS

Atg17 Is Required for Normal Autophagosome Formation

In a previous article, we reported that a null mutation of *ATG17* affected autophagy, but not the Cvt pathway (Kamada *et al.*, 2000). In wild-type cells, autophagic bodies were accumulated in the vacuole under starvation conditions in the presence of phenylmethylsulfonyl fluoride (PMSF), which prevents the disruption of autophagic bodies (Figure 1A; Takeshige *et al.*, 1992). In contrast, no visible autophagic bodies were observed in *atg17*Δ cells under starved conditions. The *atg17* mutant was complemented by the plasmid-borne copy of *ATG17*.

We also examined the autophagic activity using an assay system, in which a truncated form of proalkaline phosphatase (ALP) expressed in the cytoplasm is delivered to the vacuole in an autophagy-dependent manner (Noda *et al.*, 1995). In this assay, *atg17*Δ mutant cells exhibited defective autophagy, as seen in typical mutants in the autophagic pathway, and they also showed the loss of viability phenotype under nitrogen starvation like typical *atg* mutants (Figure 1, B and C; Tsukada and Ohsumi, 1993; Noda *et al.*, 2000).

The proform of Ape1 (prApe1) transits to the vacuole for maturation by two pathways; the Cvt pathway is utilized under vegetative growth conditions, and autophagy takes place during starvation. Even though autophagy is defective in the *atg17*Δ mutant, we found that prApe1 import occurred under starvation conditions in *atg17*Δ cells (Figure 1B; Kamada *et al.*, 2000; Nice *et al.*, 2002).

Thus, we assumed that the autophagosome-like structures enclose prApe1 and deliver it to the vacuole in starved *atg17*Δ cells. We examined the structures by electron microscopy (Figure 1D). In agreement with previous study, in a *pep4*Δ single mutant strain, normal-sized autophagic bodies (300–900 nm) were accumulated in the vacuole lumen (Figure 1D, right panel; Baba *et al.*, 1997). However, when *atg17*Δ *pep4*Δ double mutant cells were incubated under nitrogen starvation conditions for 4 h, there was no substantial accumulation of autophagic bodies inside the vacuole, like other autophagy defective mutants, such as *atg8*Δ (unpublished data; Kirisako *et al.*, 1999). Intriguingly, abnormally small autophagosomes and autophagic bodies were occasionally observed in the cytoplasm or the vacuole, respectively (Figure 1D, left panel). These structures had a diameter of ~200 nm and contained cytoplasmic ribosomes, indicating that the structures were autophagosomes. These autophagosomes were larger than and was clearly different from Cvt vesicles, which have a diameter of 140–160 nm and contain exclusively the Cvt complex (Baba *et al.*, 1997). In addition, the most of small autophagosomes sequestered the Cvt complex with quite high rate (see Figure 1D, left panel, indicated by arrowheads). It is likely that the small autophagic bodies might be sufficient to transport the Cvt complex to the vacuole, but insufficient to transport bulk cytoplasmic components. Taken together, these findings indicate that Atg17 function is required to generate properly sized-autophagosomes.

Atg1-Atg13 Binding Was Observed in atg17*-null Mutant Cells*

Our observations with electron microscopy demonstrated that the *atg17*Δ mutant allowed the formation of only a few small autophagosomes. It was shown that Atg1-Atg13 association is required for autophagy but not for the Cvt pathway (Kamada *et al.*, 2000). To test whether a physical association between Atg1 and Atg13 is still detected in *atg17*Δ cells, we carried out coimmunoprecipitation experiments. YEPD-grown cells haboring an integrated HA-tagged *ATG1* (^{HA}*ATG1*) (wild-type; YYK422 or *atg17*Δ; YYK416, see Table 1) *ATG13* via a low copy (CEN) plasmid were converted to spheroplasts and treated with 0.2 μg/ml rapamycin for 1 h. The total lysate from the spheroplasts was subjected to immunoprecipitation analysis using anti-HA antibody. Atg13 was hyperphosphorylated in a Tor-dependent manner in rich medium conditions. This form of Atg13 has a low affinity for Atg1 (Figure 2, lane 1; Kamada *et al.*, 2000). Rapamycin treatment, which inhibits Tor, resulted in dephosphorylation of Atg13, and dephosphorylated Atg13 showed a higher affinity for Atg1 (Figure 2, lane 3). Although the phosphorylated Atg13 was normally observed in *atg17*Δ cells, Atg1 associated with Atg13 not only under starvation condition but also under nutrient-rich condition (Figure 2, lanes 5 and 6). It should be noted that association of Atg1 and Atg13 is insufficient to induce autophagy. Overexpression of Atg13 results in constitutive binding between Atg1 and Atg13 even under nutrient-rich conditions (Kamada *et al.*, 2000), but it does not induce autophagy. These results suggest that binding of Atg17 with the Atg1-Atg13 complex is required for autophagy.

Atg17 Interacts with Atg1 through Atg13 under Starvation Conditions

Next, we sought to determine whether Atg17 directly interacts with the Atg1-Atg13 complex. For further biochemical analyses of Atg17, we constructed cells that had chromosomally integrated N-terminally FLAG-tagged *ATG17*

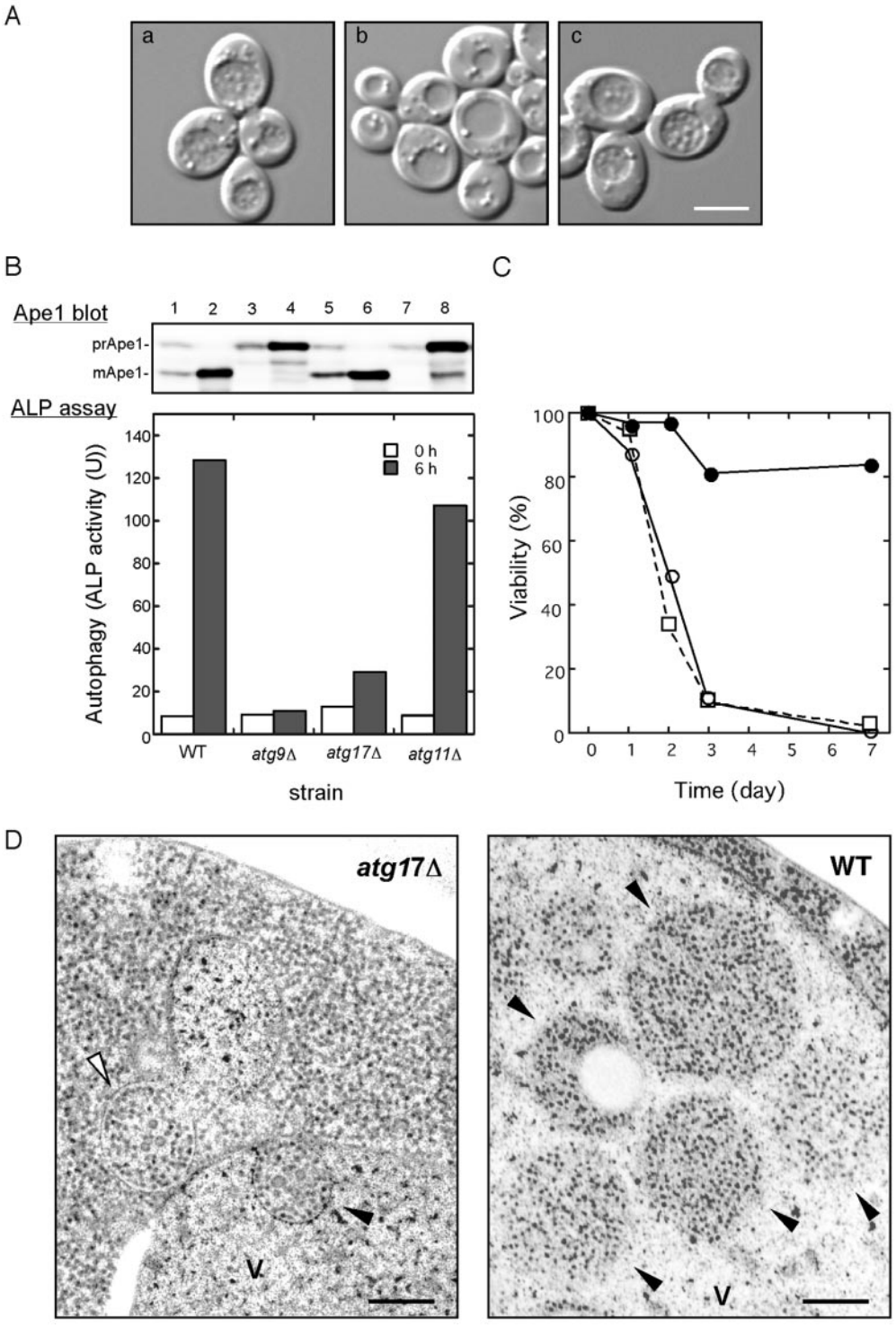

Figure 1. *ATG17* is essential for normal autophagosome formation. (A) *ATG17*-null mutant appears devoid of autophagic bodies in the vacuole. Wild-type (KVY55; a) and *atg17*Δ (YYK382) strains transformed with either vector alone (b) or the multicopy ATG17 plasmid (c) were incubated for 4 h under nitrogen and carbon starvation condition in the presence of 1 mM PMSF. DIC images are shown. Bar, 5 μm. (B) The *atg17*Δ strain blocks autophagy. Wild-type (KVY55), *atg9*Δ (YTS007), *atg17*Δ (YYK382), and *atg11*Δ (YYK475) cells in YEPD (lanes 1, 3, 5, and 7) or in SD(-N) for 4 h (lanes 2, 4, 6, and 8) were analyzed by anti-Ape1 immunoblot (top). The autophagic activity was measured by the ALP assay before (□) and after (■) nitrogen starvation for 6 h (bottom). (C) The *atg17*Δ strain is sensitive to nitrogen starvation. Wild-type (KA311A, ●), *atg1*Δ (YYK36, ○), and *atg17*Δ (YYK111, □) cells were cultured in nitrogen starvation medium. Aliquots were removed at the indicated times and spread onto YEPD plates. The number of colonies was determined after 2–3 d. (D) Deletion of *ATG17* causes formation of aberrantly small autophagosomes. The *pep4*Δ *atg17*Δ cells (YYK381; left) grown to log phase in YEPD were incubated in SD(-N) for 4 h and subjected to electron microscopy. Small autophagosome (opened arrowhead) and autophagic body (closed arrowhead) are detected in the cytoplasm and the vacuole (V), respectively. Note that the Cvt complex is contained in both autophagosome and autophagic body (left panel). Right panel shows normal autophagic bodies of wild-type cell. Bar, 200 nm.

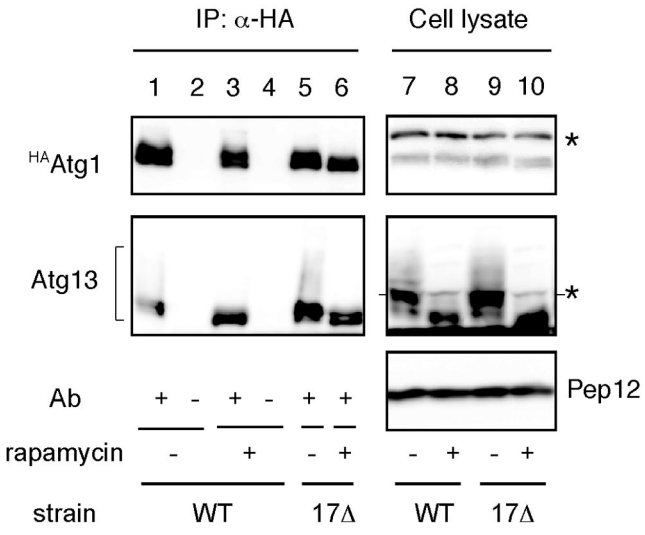

Figure 2. The interaction between Atg1 and Atg13 was not affected by *atg17*Δ. ^{HA}*ATG1* integrated cells (wild-type [WT], YYK422; or *atg17*Δ [17Δ; YYK 416]) additionally expressing Atg13 via a low-copy plasmid were enzymatically converted to spheroplasts and treated with 0.2 μg/ml rapamycin for 1 h. The total lysates were immunoprecipitated with anti-HA antibody and immunoblotted with anti-HA and anti-Atg13 antibodies. The asterisks show nonspecific bands in the total lysate that were recognized by anti-HA and -Atg13 antibodies. Immunoblot with anti-Pep12 antibody (Sigma) was carried out to monitor amount of cell lysate.

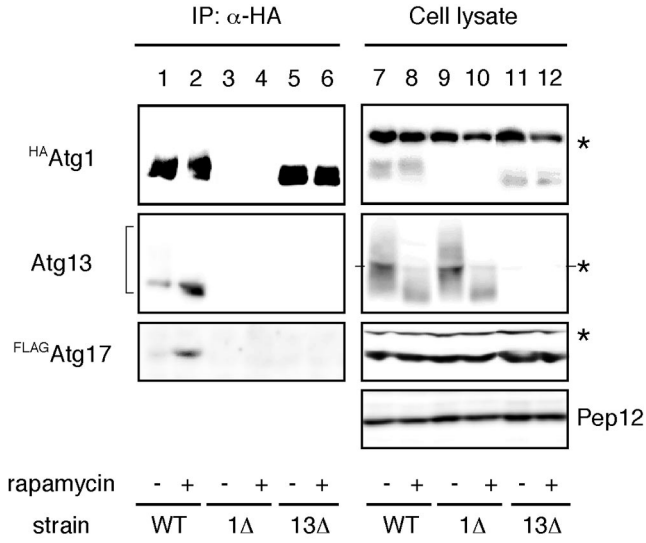

Figure 3. Atg17 interacts with Atg1 in an Atg13-dependent manner. Wild-type cells (YYK422), *atg1*Δ (YYK424) harboring a pATG13 CEN plasmid, and *atg13*Δ cells (YYK 426) were treated with rapamycin as shown in Figure 2. ^{HA}Atg1 was immunoprecipitated with anti-HA antibody and immunoblotted with anti-HA, Atg13, and Atg17 antibodies. Asterisks indicate nonspecific bands. Pep12 indicates that the amount of cell lysate per lane is equal.

(^{FLAG}*ATG17*) in addition to ^{HA}*ATG1* (YYK422). Total lysates from cells treated with or without rapamycin were subjected to immunoprecipitation with anti-HA antibody. Hyperphosphorylated Atg13 was dephosphorylated in response to rapamycin treatment, and the dephosphorylated Atg13 was efficiently coimmunoprecipitated with ^{HA}Atg1 (Figure 3, middle panel, compare lane 2 with lane 1). When the precipitated proteins were immunoblotted using antibody against Atg17, ^{FLAG}Atg17 was detected in the immunocomplex (Figure 3, lower panel, lanes 1 and 2). The amount of ^{FLAG}Atg17 bound to ^{HA}Atg1 strikingly increased in the cells treated with rapamycin for 1 h, though the amount of Atg proteins was not changed by rapamycin treatment (Figure 3, lanes 7 and 8). These results imply that Atg17 associates with the Atg1-Atg13 complex, and this association is negatively regulated by Tor.

We next examined whether Atg13 is required for the interaction between Atg1 and Atg17. In rapamycin-treated *atg13*Δ cells, no ^{FLAG}Atg17 was detected in the immunocomplex of ^{HA}Atg1 (Figure 3, lanes 5 and 6), though ^{FLAG}Atg17 was normally expressed (Figure 3, lanes 11 and 12). This implies that Atg13 is essential for the association between Atg1 and Atg17.

Atg17 Interacts with Atg13 *under Starvation Conditions*

The immunoprecipitation analysis in Figure 3 indicates that Atg17 interacts either directly with Atg13 or with Atg13 via Atg1. We examined the relationship between Atg17 and Atg13 by two-hybrid analysis. The two-hybrid interaction between Atg13 and Atg17 seen in the wild-type strain was also observed in an *atg1*Δ strain (unpublished data). The interaction between Atg13 and Atg17 was independent of the binding of Atg1 to Atg13.

Next, we examined the in vivo interaction between Atg13 and Atg17. When Atg13 was immunoprecipitated with anti-Atg13 antibody, ^{FLAG}Atg17 was coprecipitated (Figure 4, lanes 1 and 2). A stronger interaction was observed under rapamycin treatment, indicating Atg13-Atg17 association is also controlled by Tor. This association was normally detected in the *atg1*Δ cells (Figure 4, lanes 3 and 4), thus the interaction between Atg13 and Atg17 does not require Atg1.

A Mutation in ATG17 *Abolishes Complex Formation*

To address the requirement for the interaction of Atg17 with Atg1-Atg13 complex in autophagy, we decided to generate

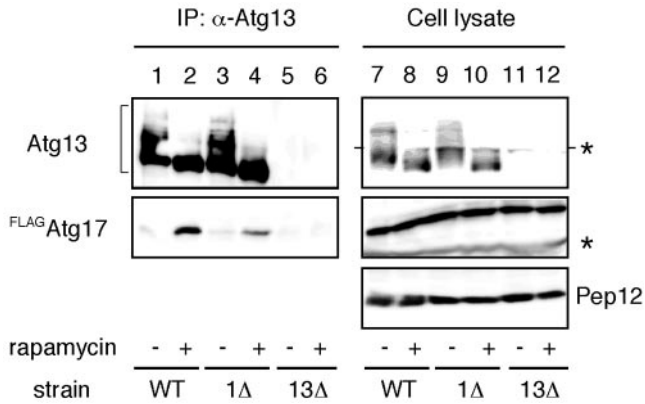

Figure 4. Atg17 interacts with Atg13 under starvation conditions. Both wild-type (YYK422) and *atg1*Δ (YYK 424) cells, which harbor additionally expressed Atg13 via a low-copy plasmid, were integrated with ^{FLAG}Atg17. The cells were grown in YEPD medium and were treated with rapamycin. Atg13 was immunoprecipitated with anti-Atg13 antibody. Associated proteins were visualized by immunoblotting with anti-Atg13 and FLAG antibodies. The asterisks indicate nonspecific bands. Equal amount cell lysate was loaded on the gel by monitoring with Pep12.

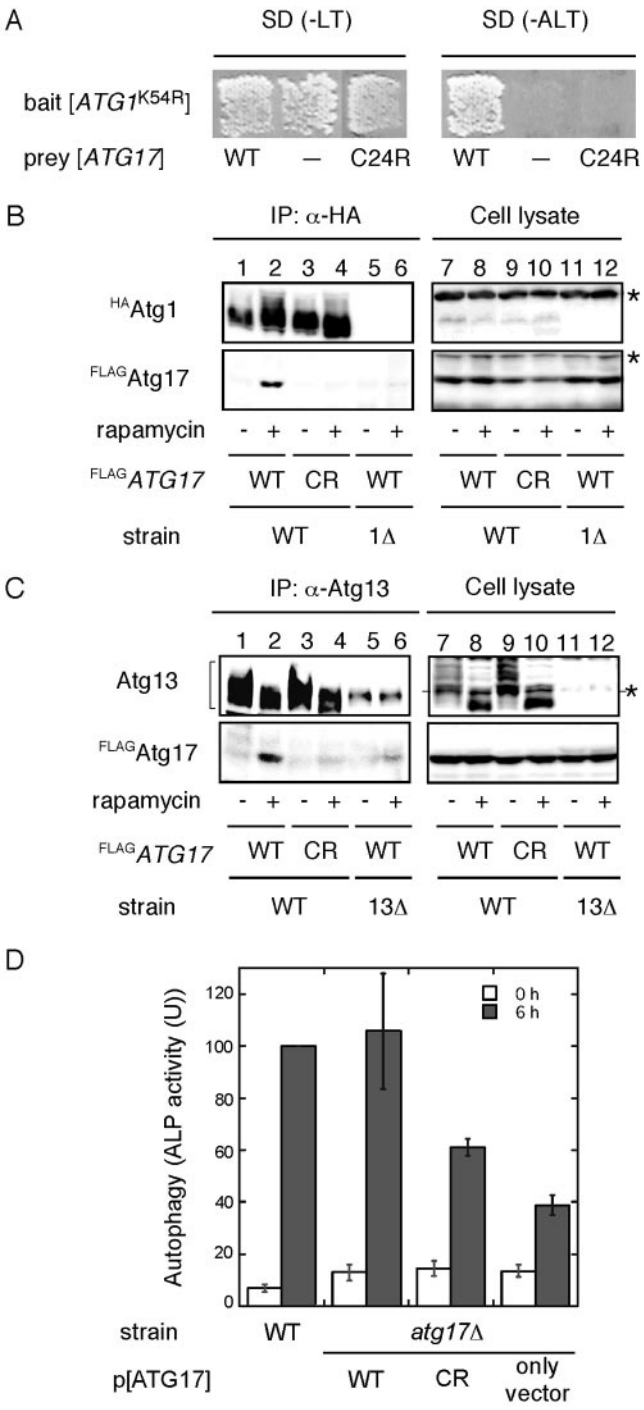

Figure 5. A mutation in *ATG17* abolishes complex formation and defects in autophagy. (A) *atg17* mutant screened by the two-hybrid system. Plasmids transformed into PJ69–4A strains are indicated. The cells were grown on SC-Leu-Trp plate (left panel), replica-plated on SC-Ade-Leu-Trp plate (right panel), and then incubated at 30°C for 3 d. (B) Atg17^{C24R} does not bind Atg1. Total lysates were prepared from wild-type cells (YYK422) and *atg17*^{C24R} cells (YYK 467) chromosomally integrated with either ^{HA}*ATG1* and ^{FLAG}*ATG17* (WT) or ^{HA}*ATG1* and ^{FLAG}*atg17*^{C24R} (CR). The cells were grown in YEPD in the absence or presence of rapamycin. The lysates were immunoprecipitated with anti-HA antibody and immunoblotted with anti-Atg17 and anti-HA antibodies. (C) Atg17^{C24R} shows reduced affinity for Atg13. Immunoprecipitation with anti-Atg13 antibody was carried out as described in Figure 4 using wild-type cells (YYK422), *atg17*^{C24R} cells (YYK 467) harboring pRS316[*ATG13*], or *atg13*Δ cells (YYK 426). After SDS-PAGE, immunoprecipitates were subjected to immunoblot analysis using anti-Atg13 or anti-FLAG antibody as indicated. The asterisk indicates a nonspecific band. (D) *atg17*^{C24R} mutant is defective for autophagy. KVY55 cells (*pho8::pho8Δ60*) or YYK382 cells (*atg17Δ pho8::pho8Δ60*) harboring the wild-type *ATG17* or *atg17*^{C24R} mutant on 2-μ plasmids were grown to 1 OD_{600}/ml in YEPD medium and then transferred to SD(-N) medium. Lysates from the cells before (0 h, □) and after 6-h starvation (■) were used for the ALP assay. The error bars indicate the SD of three independent experiments.

atg17 mutants that lack the ability to bind Atg1-Atg13 complex. Accordingly, we performed two-hybrid screening with mutagenized pGAD[*ATG17*] plasmid. Because *ATG17* was first identified through a two-hybrid screening with pGBD[*ATG1*^{K54R}] as bait (Kamada *et al.*, 2000), we used the same two-hybrid assay system. As a result, a unique candidate which was unable to bind to Atg1 was obtained from the screening. This mutant contained single point mutation, in which Cys 24 was substituted to Arg (*atg17*^{C24R}), caused a loss of the interaction with Atg1 (Figure 5A).

With the *atg17*^{C24R} mutant, we examined the interaction with Atg1-Atg13 complex by immunoprecipitation experiment. Cells with an integrated FLAG-tagged *atg17*^{C24R} gene at the *ATG17* locus (YYK467) were constructed. ^{FLAG}Atg17^{C24R} mutant protein was normally expressed as well as wild-type ^{FLAG}Atg17 (Figure 5, B and C, lanes 7–10). In an agreement with two-hybrid results, the interaction between ^{FLAG}Atg17^{C24R} mutant protein and ^{HA}Atg1 was not observed even under rapamycin treatment condition (Figure 5B, lanes 3 and 4), whereas wild-type ^{FLAG}Atg17 was coimmunoprecipitated with ^{HA}Atg1 (Figure 5B, lane 2). Moreover, ^{FLAG}Atg17^{C24R} had strikingly reduced affinity for Atg13 in the coimmunoprecipitation experiment with anti-Atg13 antibody (Figure 5C, lanes 3 and 4), suggesting a weak interaction between the Atg17^{C24R} mutant and Atg13 causes a defect in Atg1-Atg13-Atg17 complex formation.

The level of autophagic activity was examined by an ALP assay. The *atg17*Δ *pho8*Δ*60* strain (YYK382) showed lower level (below 40% of wild-type) of phosphatase activity after 6 h nitrogen starvation (Figure 5D). Expression of *ATG17* from a high-copy (2 μ) plasmid complemented the autophagic activity defect of *atg17*Δ cells (Figure 5D). However, cells expressing the Atg17^{C24R} mutant protein significantly reduced the level (about half to 60% of wild-type activity) in autophagic activity (Figure 5D). Taken together, the analysis of Atg17^{C24R} mutant protein along with two-hybrid studies suggested that the complex formation by Atg1, Atg13, and Atg17 is essential for autophagosome formation.

Interaction between Atg13 and Atg17 Is Required for Atg1 Kinase Activity

To further investigate potential role of the Atg1-Atg13-Atg17 complex, Atg1 kinase assay was performed. In a previous article, we demonstrated that Atg1 kinase activity is required for autophagy (Kamada *et al.*, 2000). However, Abeliovich *et al.* (2003) recently showed that Atg1 kinase activity is not needed for autophagy using chemical genetics. They made an amino acid substitution within the ATP-binding site of Atg1 (Atg1^{M102A}) that resulted in specific sensitivity to the ATP analog, 1-NA-PP1. They treated ATG1^{M102A} cells with this drug and observed that Ape1 transport in growing cells was inhibited by 1-NA-PP1, but this inhibition was cleared under nutrient starvation. To reexamine their results, we performed the same analysis.

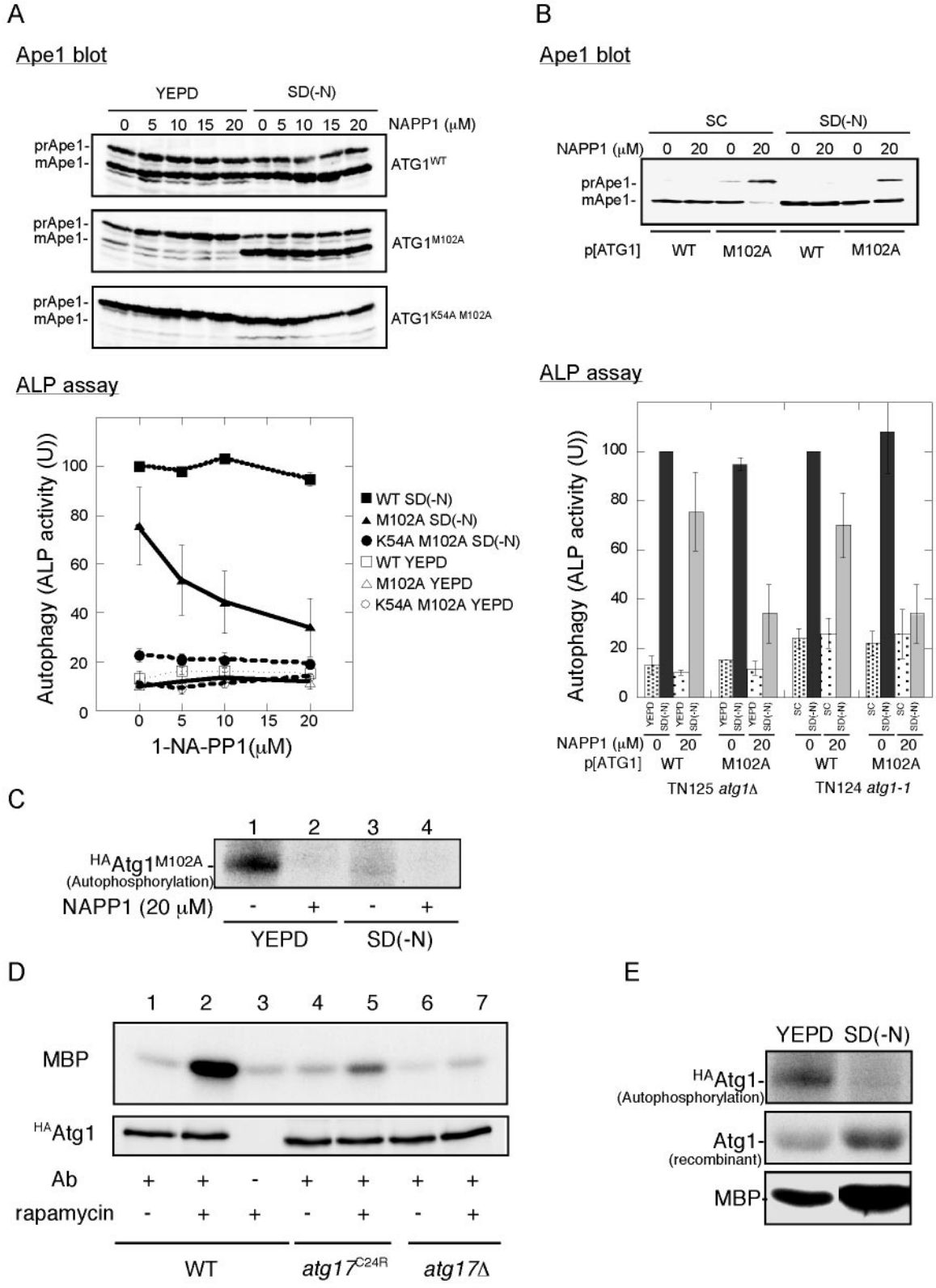

Figure 6. Interaction between Atg13 and Atg17 is required for Atg1 kinase activity. (A) Chemical genetic analysis of ATG1 using YEPD-grown cells. Cells (YYK126, *atg1*Δ *pho8*Δ60) harboring the indicated *ATG1* plasmids were grown in YEPD medium, and the cells were pretreated with 1-NA-PP1 (DMSO solution) at the indicated concentrations for 1 h. The control cells were treated with DMSO. The cells were then transferred to SD(-N) medium containing the same concentration of 1-NA-PP1 or they continued growing in YEPD for 4 h. The cells were collected and subjected to Ape1 blotting (top) or ALP assay (bottom). The percentage of ALP activity relative to that of starved control cells is shown. The values represent averages of four independent experiments, with the SD as error bars. (B) Chemical genetic analysis of *ATG1* using SC-grown cells. Cells (TN124–1C, *atg1-1 pho8*Δ*60*) harboring the indicated *ATG1* plasmids were grown in SC-Ura medium. The

We treated YEPD-grown ATG1^{M102A} cells with 1-NA-PP1 and then transferred the cells into nitrogen-depleted medium. We basically confirmed the results of Abeliovich *et al.* (2003) on the Cvt pathway (Figure 6A). Ape1 maturation in YEPD-grown cells was largely affected by addition of 1-NA-PP1, whereas Ape1 maturation in nitrogen-starved cells was normal. We noted that 1-NA-PP1 did not affect wild-type cells, suggesting that this effect was caused by the inhibition of Atg1^{M102A} by 1-NA-PP1.

Moreover, we found that 1-NA-PP1 also inhibited autophagy (Figure 6A, ALP assay). Abeliovich *et al.* (2003) reported that autophagy was not affected by a dose of 30 μM 1-NA-PP1. In our hands, 5 μM 1-NA-PP1 was enough for significant inhibition, and autophagic activity was decreased to 34% of wild-type (vehicle alone) at 20 μM 1-NA-PP1. We next tested 1-NA-PP1 sensitivity using the same strain background (TN124) just Abeliovich *et al.* had used, and we grew the cells on synthetic medium, because we thought that uptake (and thus sensitivity) of 1-NA-PP1 might differ because of strain background or growing conditions. The results are shown in Figure 6B. We again observed that 1-NA-PP1 affected both the Cvt pathway and autophagy, although autophagic activity was not completely diminished. We assume that this is the reason mature Ape1 was detected in 1-NA-PP1–treated starved cells. To confirm that Atg1^{M102A} has 1-NA-PP1–sensitive activity, we performedan in vitro autophosphorylation assay. Consistent with the autophosphorylation experiment reported by Abeliovich *et al.*, Atg1 autophosphorylation level was strikingly reduced in the presence of 1-NA-PP1 (Figure 6C). With these above reexaminations, we conclude that Atg1 kinase activity is indeed essential for the Cvt pathway and autophagy.

Finally, we examined Atg1 kinase activity in cells with integrated ^{HA}*ATG1* and either ^{FLAG}*ATG17* or ^{FLAG}*atg17*^{C24R} mutant. ^{HA}Atg1 was precipitated with anti-HA ascites fluid and the resultant immunocomplex was analyzed using an in vitro kinase assay with myelin basic protein as a substrate. As reported previously, Atg1 kinase activity was increased by starvation; therefore, the level of Atg1 kinase activity seems to be important for the regulation of autophagosome formation (Figure 6D, lanes 1 and 2; Kamada *et al.*, 2000). The increase in Atg1 kinase activity was dramatically reduced in the *atg17*^{C24R} mutant cells (Figure 6D, lane 5), suggesting that the weak interaction between the atg17^{C24R} mutant and Atg13 resulted in lower kinase activity. Therefore, stable Atg1-Atg13-Atg17 complex formation under starvation conditions is needed for full activation of Atg1 and subsequently normal autophagosome formation.

Figure 6 (facing page) cells were treated with 1-NA-PP1, incubated in SD(-N) medium, and analyzed as described in A. The values (values of the starved control cells were normalized to 100%) represent the mean ALP activities from four independent experiments. The results from YEPD-grown cells (shown in A) are also shown. (C) Autophosphorylation activity of Atg1^{M102A} is inhibited by 20 μM 1-NA-PP1. Cell extract of the ^{HA}Atg1^{M102A} mutant cells before (left) and after (right) nitrogen starvation for 4 h was immunoprecipitated with anti-HA antibody, and the resultant immunocomplex was assayed for autophosphorylation activity in the presence of or absence of 20 μM 1-NA-PP1. (D) Atg1 kinase activity is impaired in *atg17*^{C24R} mutant cells. Wild-type (YYK422), *atg17*^{C24R} mutant (YYK467), or *atg17*Δ mutant (YYK416) cells were treated with rapamycin (0.2 μg/ml, 30 min) and subjected to Atg1 kinase assay. (E) Atg1 kinase activity in phosphorylating itself is increased in starvation condition. ^{HA}Atg1^{WT}, immunoprecipitated as described in C, was subjected to autophosphorylation assay (top), to protein kinase assay using 4 μg of recombinant Atg1 protein as a substrate (middle), and to protein kinase assay using 4 μg of myelin basic protein (MBP, bottom).

DISCUSSION

Autophagy and the Cvt pathway are distinct membrane trafficking processes that nonetheless share most of their mechanistic components. To gain further insight into factors that distinguish between these pathways, we have examined a protein, Atg17, which is required specifically for autophagy. Here, we have first demonstrated that Atg17 function is required to maintain proper size of autophagosome. With the light microscopy, autophagosomes were invisible in the *atg17* null mutant. But here we found a few and small autophagosomes by electron microscopy, which may be hardly detectable by a light microscope, would be built up in the absence of Atg17. The other steps in the autophagy, such as vesicle nucleation, cargo sequestration, docking, and fusion to the vacuole, seemed normal. The size of the autophagosomes (~200 nm in diameter) seen in the *atg17*Δ cells was abnormally small compared with normal autophagosomes (300–900 nm in diameter). These smaller autophagosomes must not engulf or transport a sufficient amount of cytosolic components to allow cells surviving under starvation conditions. However, the aberrant small autophagosomes efficiently enwrapped the Cvt complex containing prApe1. As a result, prApe1 import is only minimally affected in either growth or starvation conditions in the *atg17*Δ cells (Kamada *et al.*, 2000; Nice *et al.*, 2002). According to the current model, the preautophagosomal structure (PAS) seems to play a pivotal role in autophagosome formation (Suzuki *et al.*, 2001). The deletion of *ATG17* does not affect PAS formation, but does affect subsequent autophagosome formation (Suzuki *et al.*, 2001, 2004). The results by electron microscopy explain why *ATG17* is indispensable for autophagy but not for the Cvt pathway and suggest that Atg17 functions in the expansion of autophagosomes to the normal size.

Next, we have demonstrated that Atg1, Atg13, and Atg17 form a protein complex in response to nutrient starvation. It is noteworthy that not only Atg1 and Atg13 association (Kamada *et al.*, 2000), but also Atg13 and Atg17 association is regulated by Tor. Abeliovich *et al.* (2003) reported that Atg1 and Atg13 binding was not detected when these proteins were expressed at a chromosomal level. We conducted coimmunoprecipitation experiment with YYK422, in which Atg1, Atg13, and Atg17 were expressed at a chromosomal level. Atg13 and ^{FLAG}Atg17 were coprecipitated with ^{HA}Atg1 in response to rapamycin treatment, although it was not easy to detect the low levels of Atg13 in the cell lysates (unpublished data). To improve the detection of Atg13, we used cells harboring a centromeric (CEN) plasmid containing *ATG13* in addition to chromosomal *ATG13* in this study.

In the presence of rapamycin, association of Atg1 with dephosphorylated Atg13 was normally detected in *atg17*Δ cells, but did not cause upshift of Atg1 kinase activity, leading to the production of abnormal autophagosomes. It is likely that Atg17 regulates Atg1 kinase activity in concert with Atg13, and the activation of Atg1 kinase activity is important for autophagosome formation. These conclusions are in agreement with our previously reported results (Kamada *et al.*, 2000). At this moment, *ATG17* function under nutrient-rich condition is unclear, because it is not needed for the Cvt pathway. Our finding that Atg1 associates with Atg13 in *atg17*Δ cells under nutrient-rich condition may produce a clue to elucidate Atg17 function in growing cell.

For instance, Atg17 might prevent the association between Atg1 and Atg13 under nutrient-rich conditions.

It turns out that the interaction between Atg1 and Atg17 is mediated by Atg13. In two-hybrid analysis we saw that Atg17 bound to Atg1 even in *atg13*Δ cells (unpublished data), so it still remains possible that Atg17 itself possesses an Atg1-binding site and directly interacts with Atg1. The interaction between Atg17 and Atg13 is enhanced by treatment with rapamycin, which was not dependent on Atg1. The phosphorylation state of Atg13 is under the control of Tor, which regulates Atg1 and Atg13 association. Thus, Atg17 might possess a higher affinity for dephosphorylated Atg13 than for the hyperphosphorylated Atg13. It still remained possible that Atg17 is another target of Tor signaling.

We also obtained the *atg17*^{C24R} mutant, which has a defect in interaction with Atg13. Though putative domains and functional motifs are not known in the Atg17 sequence, our finding discerns that Cys24 is likely to require for binding to Atg13. The unstable interaction between Atg17^{C24R} and Atg13 results in both decreased autophagic activity and decreased Atg1 kinase activity. These data indicate that the activated Atg1 kinase activity by dephosphorylated Atg13 in our previous findings (Kamada *et al.*, 2000) is dependent on the interaction between Atg17 and Atg13.

Klionsky and his colleagues recently studied *ATG1* using chemical genetic analysis and reported that Atg1 kinase activity is dispensable for autophagy (Abeliovich *et al.*, 2003). Their conclusion completely disagrees with our previous results. Therefore, we precisely reexamined the chemical genetic analysis, and we found that Atg1 kinase activity is indeed needed for autophagy. We also found that the phenotype of 1-NA-PP1–treated starved cells resembles that of *atg17*Δ cells. Both cells have autophagic defects, although Ape1 seems to be normally transported to the vacuole. We assume this is why Abeliovich *et al.* observed autophagosomes in rapamycin and 1-NA-PP1–treated ATG1^{M102A} cells. In previous article (Matsuura *et al.*, 1997), we observed that in vitro autophosphorylation of Atg1 was apparently decreased during starvation (Figure 3, D and E, in Matsuura *et al.*, 1997). There we discussed that Atg1 isolated from starved cells was already autophosphorylated in vivo, and that is why ^{32}P label was less incorporated in Atg1 from starved cell than that from growing cell. We performed in vitro Atg1 kinase assay with recombinant Atg1 protein as a substrate, and we observed that Atg1 immunopurified from starved cell transferred ^{32}P label to the substrate better than Atg1 from a growing cell (Figure 6E), supporting our explanation. However, Abeliovich *et al.* interpreted this data that intrinsic kinase activity of Atg1 is decreased, and they claimed in their article that Atg1 is down-regulated under starvation condition.

To date, we have found three Atg1-binding proteins, Atg13 and Atg17, which are indispensable for autophagy, and Atg11/Cvt9, which is not necessary for autophagy. Atg1 kinase activity is largely impaired in *atg13*Δ or *atg17*Δ mutant cells, whereas it is not affected in *atg11*Δ cell (Kamada *et al.*, 2000). In our mutant collection, we have 21 *atg1* alleles. Among these alleles, 14 express the full-length Atg1 protein, and at least 11 alleles have point mutations in the conserved kinase region, such as Ala235, P236, and E237 (in the conserved region in subdomain VIII), and D249 and G254 (in subdomain IX; unpublished data). Considering these accumulated data, we think it is reasonable to believe that Atg1 kinase activity is essential for autophagy.

We are now able to propose a model for the signal transduction pathway of autophagy. In step 1, Tor inactivation is caused by starvation or rapamycin treatment and immediately promotes the dephosphorylation of Atg13 (Kamada *et al.*, 2000). In step 2, Atg17 binds to dephosphorylated Atg13. In step 3, the Atg13-Atg17 complex associates with Atg1, leading to the stimulation of Atg1 kinase activity by the Atg13-Atg17 complex. These processes are required for the normal progression of autophagy.

Genome wide systematic two-hybrid analysis of the *S. cerevisiae* genome suggests that Atg17 interacts with numerous proteins required for several cellular processes (Drees *et al.*, 2001). These interactions include association with Atg17 itself. Coimmunoprecipitation experiments indicated that Atg17 molecules can physically interact with each other (unpublished data). The majority of Atg17 (49 kDa) seems to be present in an >440-kDa fraction in exclusion chromatography experiments (Kabeya, Kamada, and Ohsumi, unpublished data). Recently, Atg17 was found to interact with two Cvt pathway–specific components, Atg24/Cvt13/Snx4 and Atg20/Cvt20, proteins that contain PtdIns(3)P-binding PX domains (Uetz *et al.*, 2000; Nice *et al.*, 2002). It remains a challenge to evaluate the meaning of interactions between the autophagic-specific Atg17 protein and Cvt pathway-specific Atg24 and Atg20 proteins.

Here, we define an Atg17 complex, which includes Atg1 and Atg13 and which forms in response to nutrient conditions. This complex functions in the expansion of autophagosomes to their normal size. Further analysis of Atg17 and Atg17-associated proteins will provide further information about the mechanism that modulates specificity in autophagy.

ACKNOWLEDGMENTS

We thank P. James (University of Wisconsin) for providing the yeast strain and vectors for the two-hybrid analysis; D. J. Klionsky (University of Michigan) for protein A fused Atg17 plasmid with CUP1 promoter; N. N. Suzuki, Y. Fujioka, and F. Inagaki (Hokkaido University) for recombinant Atg1 protein; T. Sekito (in our laboratory) and T. Funakoshi (Riken, Wako, Japan) for providing strains; and the National Institute for Basic Biology Center for Analytical Instruments for technical assistance. We also thank N. Suzuki for his help and encouragement of 1-NA-PP1 synthesis. This work was supported in part by grants-in-aid for Scientific Research from the Ministry of Education, Culture, Sports, Science, and Technology of Japan.

REFERENCES

Abeliovich, H., Zhang, C., Dunn, W. A., Jr., Shokat, K. M., and Klionsky, D. J. (2003). Chemical genetic analysis of Apg1 reveals a non-kinase role in the induction of autophagy. Mol. Biol. Cell *14*, 477–490.

Baba, M., Osumi, M., Scott, S. V., Klionsky, D. J., and Ohsumi, Y. (1997). Two distinct pathways for targeting proteins from the cytoplasm to the vacuole/lysosome. J. Cell Biol. *139*, 1687–1695.

Baba, M., Takeshige, K., Baba, N., and Ohsumi, Y. (1994). Ultrastructural analysis of the autophagic process in yeast: detection of autophagosomes and their characterization. J. Cell Biol. *124*, 903–913.

Bishop, A. C., Kung, C.-y., Shah, K., Witucki, L., Shokat, K. M., and Liu, Y. (1999). Generation of monospecific nanomolar tyrosine kinase inhibitors via a chemical genetic approach. J. Am. Chem. Soc. *121*, 627–631.

Dieffenbach, C. W., and Dveksler, G. S. (1995). PCR Primer: A Laboratory Manual, Plainview, NY: Cold Spring Harbor Laboratory Press.

Drees, B. L. *et al.* (2001). A protein interaction map for cell polarity development. J. Cell Biol. *154*, 549–571.

Funakoshi, T., Matsuura, A., Noda, T., and Ohsumi, Y. (1997). Analyses of *APG13* gene involved in autophagy in yeast, *Saccharomyces cerevisiae*. Gene *192*, 207–213.

Giaever, G. *et al.* (2002). Functional profiling of the *Saccharomyces cerevisiae* genome. Nature *418*, 387–391.

Hanafeld, U., Rees, C. W., White, A.J.P., and Williams, D. J. (1996). One-pot synthesis of tetrasubstituted pyrazoles-proofs of regiochemistry. J. Chem. Soc. Perkin *1*, 1545–1552.

Hutchins, M. U., Veenhuis, M., and Klionsky, D. J. (1999). Peroxisome degradation by *Saccharomyces cerevisiae* is dependent on machinery of macroautophagy and the Cvt pathway. J. Cell Sci. *112*, 4079–4087.

Irie, K., Takase, M., Lee, K. S., Levin, D. E., Araki, H., Matsumoto, K., and Oshima, Y. (1993). *MKK1* and *MKK2*, which encode *Saccharomyces cerevisiae* mitogen-activated protein Kinase-kinase homologs, function in the pathway mediated by protein kinase C. Mol. Cell Biol. *13*, 3076–3083.

James, P., Halladay, J., and Craig, E. A. (1996). Genomic libraries and a host strain designed for highly efficient two-hybrid selection in yeast. Genetics *144*, 1425–1436.

Kaiser, C., Michaelis, S., and Mitchell, A. (1994). Methods in Yeast Genetics, Cold Spring Harbor, NY: Cold Spring Harbor Laboratory Press.

Kamada, Y., Funakoshi, T., Shintani, T., Nagano, K., Ohsumi, M., and Ohsumi, Y. (2000). Tor-mediated induction of autophagy via an Apg1 protein kinase complex. J. Cell Biol. 1507–1513.

Kirisako, T., Baba, M., Ishihara, N., Miyazawa, K., Ohsumi, M., Yoshimori, T., Noda, T., and Ohsumi, Y. (1999). Formation process of autophagosome is traced with Apg8/Aut7p in yeast. J. Cell Biol. *147*, 435–446.

Klionsky, D. J., and Ohsumi, Y. (1999). Vacuolar import of proteins and organelles from the cytoplasm. Annu. Rev. Cell Dev. Biol. *15*, 1–32.

Matsuura, A., Tsukada, M., Wada, Y., and Ohsumi, Y. (1997). Apg1p, a novel protein kinase required for the autophagic process in *Saccharomyces cerevisiae*. Gene *192*, 245–250.

Nice, D. C., Sato, T. K., Stromhaug, P. E., Emr, S. D., and Klionsky, D. J. (2002). Cooperative binding of the cytoplasm to vacuole targeting pathway proteins, Cvt13 and Cvt20, to phosphatidylinositol 3-phosphate at the pre-autophagosomal structure is required for selective autophagy. J. Biol. Chem. *277*, 30198–30207.

Noda, T., Kim, J., Huang, W. P., Baba, M., Tokunaga, C., Ohsumi, Y., and Klionsky, D. J. (2000). Apg9p/Cvt7p is an integral membrane protein required for transport vesicle formation in the cvt and autophagy pathways. J. Cell Biol. *148*, 465–479.

Noda, T., Matsuura, A., Wada, Y., and Ohsumi, Y. (1995). Novel system for monitoring autophagy in the yeast *Saccharomyces cerevisiae*. Biochem. Biophys. Res. Commun. *210*, 126–132.

Noda, T., and Ohsumi, Y. (1998). Tor, a phosphatidylinositol kinase homologue, controls autophagy in yeast. J. Biol. Chem. *273*, 3963–3966.

Robinson, J. S., Klionsky, D. J., Banta, L. M., and Emr, S. D. (1988). Protein sorting in *Saccharomyces cerevisiae*: isolation of mutants defective in the delivery and processing of multiple vacuolar hydrolases. Mol. Cell. Biol. *8*, 4936–4948.

Scott, S. V., Hefner-Gravink, A., Morano, K.A., Noda, T., Ohsumi, Y., and Klionsky, D. J. (1996). Cytoplasm-to-vacuole targeting and autophagy employ the same machinery to deliver proteins to the yeast vacuole. Proc. Natl. Acad. Sci. USA *93*, 12304–12308.

Straub, M., Bredschneider, M., and Thumm, M. (1997). AUT3, a serine/threonine kinase gene, is essential for autophagocytosis in *Saccharomyces cerevisiae*. J. Bacteriol. *179*, 3875–3883.

Suzuki, K., Kirisako, T., Kamada, Y., Mizushima, N., Noda, T., and Ohsumi, Y. (2001). The pre-autophagosomal structure organized by concerted functions of *APG* genes is essential for autophagosome formation. EMBO J. *20*, 5971–5981.

Suzuki, K., Noda, T., and Ohsumi, Y. (2004). Interrelationships among Atg proteins during autophagy in *Saccharomyces cerevisiae*. Yeast *21*, 1057–1065.

Takeshige, K., Baba, M., Tsuboi, S., Noda, T., and Ohsumi, Y. (1992). Autophagy in yeast demonstrated with proteinase-deficient mutants and conditions for its induction. J. Cell Biol. *119*, 301–311.

Thumm, M., Egner, R., Koch, B., Schlumpberger, M., Straub, M., Veenhuis, M., and Wolf, D. H. (1994). Isolation of autophagocytosis mutants of *Saccharomyces cerevisiae*. FEBS Lett. *349*, 275–280.

Tsukada, M., and Ohsumi, Y. (1993). Isolation and characterization of autophagy-defective mutants of *Saccharomyces cerevisiae*. FEBS Lett. *333*, 169–174.

Uetz, P. *et al.* (2000). A comprehensive analysis of protein-protein interactions in *Saccharomyces cerevisiae*. Nature *403*, 623–627.